The scaling transformation $(S^{-3})^T$ leaves a primitive 6D reciprocal lattice invariant as can easily be seen from its application on the indices:

$$\begin{pmatrix} h_1' \\ h_2' \\ h_3' \\ h_4' \\ h_5' \\ h_6' \end{pmatrix} = \begin{pmatrix} -2 & 1 & 1 & 1 & 1 & 1 \\ 1 & -2 & 1 & -1 & -1 & 1 \\ 1 & 1 & -2 & 1 & -1 & -1 \\ 1 & -1 & 1 & -2 & 1 & -1 \\ 1 & -1 & -1 & 1 & -2 & 1 \\ 1 & 1 & -1 & -1 & 1 & -2 \end{pmatrix}_D \begin{pmatrix} h_1 \\ h_2 \\ h_3 \\ h_4 \\ h_5 \\ h_6 \end{pmatrix}.$$

The matrix $(S^{-1})^T$ leaves $M^* = \{\mathbf{H}^{\parallel} = \sum_{i=1}^{6} h_i \mathbf{a}_i^* | h_i \in \mathbb{Z}\}$ invariant,

$$\begin{pmatrix} h_1' \\ h_2' \\ h_3' \\ h_4' \\ h_5' \\ h_6' \end{pmatrix} = \tfrac{1}{2} \begin{pmatrix} -1 & 1 & 1 & 1 & 1 & 1 \\ 1 & -1 & 1 & -1 & -1 & 1 \\ 1 & 1 & -1 & 1 & -1 & -1 \\ 1 & -1 & 1 & -1 & 1 & -1 \\ 1 & -1 & -1 & 1 & -1 & 1 \\ 1 & 1 & -1 & -1 & 1 & -1 \end{pmatrix}_D \begin{pmatrix} h_1 \\ h_2 \\ h_3 \\ h_4 \\ h_5 \\ h_6 \end{pmatrix},$$

for any $\mathbf{H} = \sum_{i=1}^{6} h_i \mathbf{d}_i^*$ with h_i all even or all odd, corresponding to a 6D face-centred hypercubic lattice. In a second case the sum $\sum_{i=1}^{6} h_i$ is even, corresponding to a 6D body-centred hypercubic lattice. Block-diagonalization of the matrix S decomposes it into two irreducible representations. With $WSW^{-1} = S_V = S_V^{\parallel} \oplus S_V^{\perp}$ we obtain

$$S_V = \left(\begin{array}{ccc|ccc} \tau & 0 & 0 & 0 & 0 & 0 \\ 0 & \tau & 0 & 0 & 0 & 0 \\ 0 & 0 & \tau & 0 & 0 & 0 \\ \hline 0 & 0 & 0 & -1/\tau & 0 & 0 \\ 0 & 0 & 0 & 0 & -1/\tau & 0 \\ 0 & 0 & 0 & 0 & 0 & -1/\tau \end{array}\right)_V = \left(\begin{array}{c|c} S^{\parallel} & 0 \\ \hline 0 & S^{\perp} \end{array}\right)_V,$$

the scaling properties in the two 3D subspaces: scaling by a factor τ in parallel space corresponds to a scaling by a factor $(-\tau)^{-1}$ in perpendicular space. For the intensities of the scaled reflections analogous relationships are valid, as discussed for decagonal phases (Figs. 4.6.3.36 and 4.6.3.37, Section 4.6.3.3.2.5).

4.6.4. Experimental aspects of the reciprocal-space analysis of aperiodic crystals

4.6.4.1. *Data-collection strategies*

Theoretically, aperiodic crystals show an infinite number of reflections within a given diffraction angle, contrary to periodic crystals. The number of reflections to be included in a structure analysis of a *periodic* crystal may be very high (one million for virus crystals, for instance) but there is no ambiguity in the selection of reflections to be collected: all Bragg reflections within a limiting sphere in reciprocal space, usually given by $0 \le \sin\theta/\lambda \le 0.7$ Å^{-1}, are used. All reflections, observed and unobserved, are included to fit a reliable structure model.

However, for *aperiodic* crystals it is not possible to collect the infinite number of dense Bragg reflections within $0 \le \sin\theta/\lambda \le 0.7$ Å^{-1}. The number of observable reflections within this limiting sphere depends only on the spatial and intensity resolution.

What happens if not all reflections are included in a structure analysis? How important is the contribution of reflections with large perpendicular-space components of the diffraction vector which are weak but densely distributed? These problems are illustrated using the example of the Fibonacci sequence. An infinite model structure consisting of Al atoms with isotropic thermal parameter $B = 1$ Å^2, and distances S = 2.5 Å and L = τS, was used for the calculations (Table 4.6.4.1).

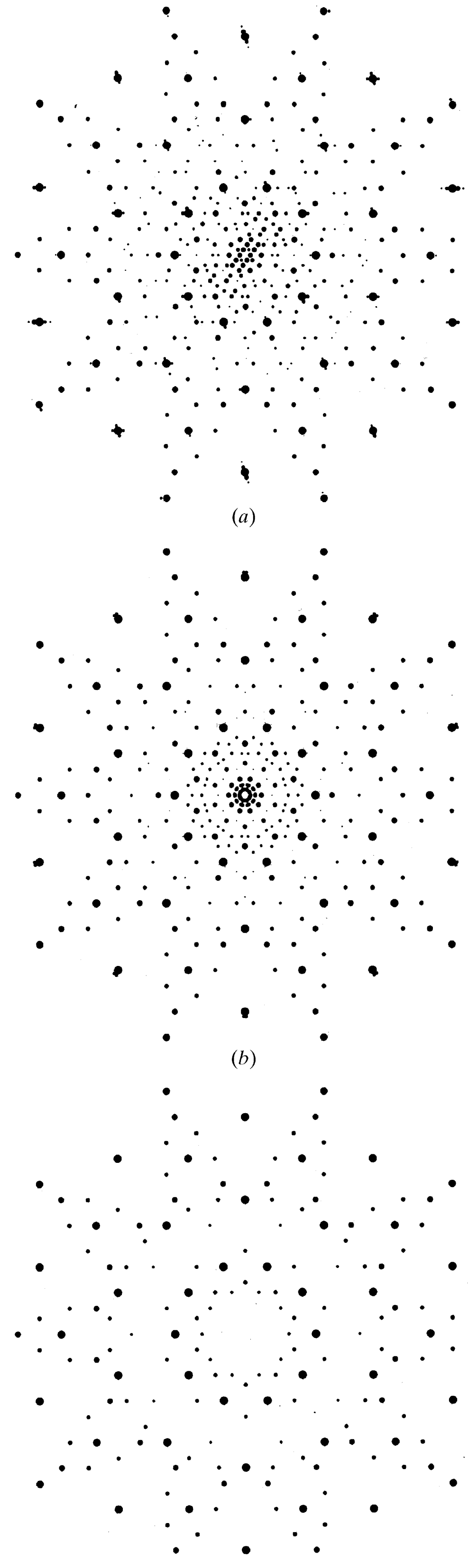

(*a*) (*b*) (*c*)

Fig. 4.6.4.1. Simulated diffraction patterns of (*a*) the $\simeq 52$ Å single-crystal approximant of decagonal Al–Co–Ni, (*b*) the fivefold twinned approximant, and (*c*) the decagonal phase itself (Estermann *et al.*, 1994).